

## Research Article

# The Role of L-arginine in Inclusion Complexes of Omeprazole with Cyclodextrins

Ana Figueiras,<sup>1,5</sup> Jorge M. G. Sarraguça,<sup>2,3</sup> Alberto A. C. C. Pais,<sup>2</sup> Rui A. Carvalho,<sup>4</sup> and J. Francisco Veiga<sup>5,6</sup>

Received 29 July 2009; accepted 22 December 2009; published online 5 February 2010

**Abstract.** In this study, we investigate how the effect of L-arginine (ARG) and cyclodextrins upon omeprazole (OME) stability and solubility. The effect of the presence of ARG on the apparent stability constants ( $K_{1:1}$ ) of the inclusion complexes formed between OME and each cyclodextrin,  $\beta$ -cyclodextrin ( $\beta$ CD), and methyl- $\beta$ -cyclodextrin (M $\beta$ CD) is studied by phase solubility diagrams and nuclear magnetic resonance (NMR) spectroscopy. The interaction of OME with those cyclodextrins, in the presence of ARG, is characterized using NMR spectroscopy and molecular dynamics simulations. ARG significantly increases the drug solubility and complex stability, in comparison to inclusion complexes formed in its absence. The effect is more pronounced for the OME: $\beta$ CD complex. ARG also contributes to a larger stability of OME when free in aqueous solution. The combination of ARG with cyclodextrins can represent an important tool to develop stable drug formulations.

**KEY WORDS:** cyclodextrins; L-arginine; molecular dynamics simulation; NMR spectroscopy; omeprazole.

## INTRODUCTION

Omeprazole (OME; Fig. 1a) is a proton pump inhibitor in gastric parietal cells. This drug has been widely used in the treatment of peptic ulcer, reflux esophagitis, and the Zollinger–Ellison syndrome (1,2). However, OME is poorly soluble in water and shows low physicochemical stability at neutral and acidic conditions (3,4). All these drawbacks give rise to difficulties in obtaining an oral pharmaceutical formulation with an acceptable bioavailability due to its rapid degradation in the stomach (5–7).

Cyclodextrins are cyclic oligosaccharides that contain a somewhat lipophilic central cavity and a hydrophilic outer surface (8). The internal hydrophobic cavity facilitates the inclusion of a number of guest molecules (9–12), and cyclodextrins have successfully been used as drug carriers to

improve drug solubility, chemical stability, dissolution, and bioavailability or to decrease unfavorable side effects (13–20).

Natural cyclodextrins have low aqueous solubility (21), and to surpass this limitation, chemically modified cyclodextrins have been synthesized with improved water solubility and greater solubilizing and complexing power than the natural cyclodextrins (22). An example is methyl- $\beta$ -cyclodextrin (M $\beta$ CD with  $r=\text{CH}_3$ , Fig. 1b), a chemically modified  $\beta$ CD (23,24). Moreover, it has been observed that the addition of suitable auxiliary substances can significantly increase the cyclodextrin complexing ability by multicomponent complex formation (25). Arginine (ARG, Fig. 1c) has been studied as an auxiliary component mainly in systems involving hydroxypropyl  $\beta$ CD (HP $\beta$ CD) as complexation agent (26–29). The use of the OME: $\beta$ CD:ARG system has been reported by other authors (30,31). The process by which the ARG acts at a molecular level in these systems has not, however, been previously addressed.

On previous studies, we have reported on the use of cyclodextrins in order to increase OME solubility (11,32). In the present study, we incorporate ARG as a third component in the formation of the inclusion complexes. The goal of the present work is to describe and explain the effects over the drug stability and solubility created by the introduction of ARG in systems where cyclodextrin inclusion complexes are formed. We also address the direct interaction between the drug and ARG. Nuclear magnetic resonance (NMR) spectroscopy is used to determine the stoichiometry and arrangement of the multicomponent inclusion complexes formed. Molecular dynamics simulations are performed with the intent of, in conjunction with the former technique, obtaining some insight on the arrangements and preferential interactions involving the components of the system.

<sup>1</sup> CICS, Centro de Investigação em Ciências da Saúde, Faculdade de Ciências da Saúde, Universidade da Beira Interior, Covilhã, Portugal.

<sup>2</sup> Departamento de Química, Faculdade de Ciências e Tecnologia, Universidade de Coimbra, Coimbra, Portugal.

<sup>3</sup> REQUIMTE, Serviço de Química-Física da Faculdade de Farmácia, Universidade do Porto, Rua Aníbal Cunha, 164, 4099-030, Porto, Portugal.

<sup>4</sup> Centro de Espectroscopia de RMN e Centro de Neurociências, Departamento de Bioquímica, Faculdade de Ciências e Tecnologia, Universidade de Coimbra, Coimbra, Portugal.

<sup>5</sup> CEF, Centro de Estudos Farmacêuticos, Departamento de Tecnologia Farmacêutica, Faculdade de Farmácia, Universidade de Coimbra, 3000-295, Coimbra, Portugal.

<sup>6</sup> To whom correspondence should be addressed. (e-mail: fveiga@ci.uc.pt)

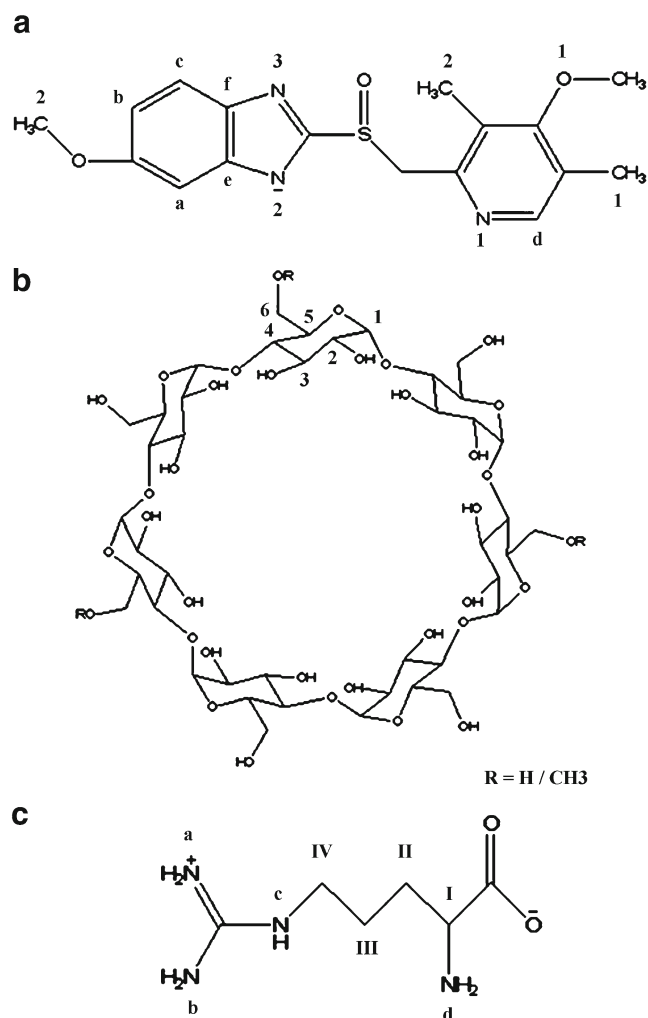


Fig. 1. Molecular structures of OME (a),  $\beta$ CD/M $\beta$ CD (b), and ARG (c)

## MATERIALS AND METHODS

### Materials

$\beta$ CD,  $M_w=1,135$  g/mol and M $\beta$ CD,  $M_w=1,190$  g/mol and an average degree of substitution, D.S.=0.5, were kindly donated by Roquette (Lestrem, France) and OME,  $M_w=345.42$  g/mol, by Belmac Laboratory, S.A. (Madrid, Spain). Deuterium oxide ( $D_2O$ ; 99.97%) was purchased from Eurisotop (Peypin, France), and triethanolamine, tris(hydroxymethyl)aminomethane, L-arginine, L-lysine, and triethylamine were supplied from Panreac (Santiago de Compostela, Spain). All other reagents were of the highest purity available from commercial sources. All products were used as received.

### Phase Solubility Studies

Phase solubility diagrams were performed using the method reported by Higuchi and Connors (33). Increasing concentrations of cyclodextrins,  $\beta$ CD (0–13.2 mM), and

M $\beta$ CD (0–42 mM) were added to excess amounts of OME, containing a fixed concentration of ARG (57.9 mM). The concentration of the alkali agent was selected in order to maintain the pH=10 in the final solutions, so as to avoid drug degradation. Suspensions were stirred at room temperature until reaching equilibrium (96 h). All suspensions were filtered through a 0.45  $\mu$ m membrane filter (Millipore), suitably diluted, and analyzed spectrophotometrically (UV-1603, Shimadzu, Japan) at 306 nm. The  $K_{1:1}$  values for the complexation were calculated using Eq. 1:

$$K_s = \text{slope}/S_0(1 - \text{slope}) \quad (1)$$

Preliminary solubility studies between OME alone and other different alkali agents (triethanolamine, tris(hydroxymethyl)aminomethane, L-lysine, and triethylamine) were performed. A direct correlation between the improvement in drug solubility and the pH of the final solutions was observed. ARG, L-lysine, and triethylamine increased the OME solubility with higher efficacy comparatively to triethanolamine and tris(hydroxymethyl)aminomethane. These alkali agents were, thus, selected to investigate the influence in drug solubility in the presence of a constant concentration of  $\beta$ CD (10 mM). When  $\beta$ CD was present, only ARG showed the ability to increase the drug solubility, with the other alkali agents OME solubility maintained or decreased. It is also noteworthy that, when  $\beta$ CD is present, the improvement in drug solubility was found not to be pH dependent suggesting that the other alkali agents compete with OME for the entrance in the cavity. For these reasons, ARG was the third component selected in this study.

### NMR Spectroscopy

$^1H$ -NMR spectra were recorded at 25°C on a Varian 500 MHz spectrometer using a 5-mm NMR probe and a simple pulse-acquire sequence with solvent presaturation. Acquisition parameters consisted of 24 k points covering a sweep width of 8 kHz, a pulse width of 18  $\mu$ s, and a total repetition time of 15 s. Digital zero filling to 64 k and a 0.5 Hz exponential were applied before Fourier transformation.

$K_{1:1}$  values were determined by NMR spectroscopy. Sample solutions were prepared by dissolving pure materials in 600  $\mu$ L of  $D_2O$  in order to maintain constant concentrations of OME (3 mM) and ARG (10 mM) and changing cyclodextrin concentration in a molar ratio relatively to drug concentration from 1:0.1 until 1:7 (OME:cyclodextrin). Chemical shifts variations ( $\Delta\delta$ ) caused by complexation were measured. A nonlinear least squares procedure resorting to the Levenberg–Marquardt algorithm (34) on the differences observed in the chemical shifts due to the presence of cyclodextrins was used in order to estimate and compare the values of  $K_{1:1}$  of the inclusion complexes obtained by different methodologies.

To determine the arrangement of the multicomponent inclusion complexes, prepared by freeze-dried method, samples were dissolved to obtain an OME final concentration of 6 mM. In the preparation of the inclusion complexes, cyclodextrins and ARG were added in a proportion 1:1 and 6:1, respectively, according to phase solubility studies that indicate an increase in OME solubility with the amount of ARG. This

proportion produces a  $\text{pH} \sim 10$ , which was imposed as an upper limit. Reference solutions were prepared by separately dissolving an appropriate amount of OME, ARG, and cyclodextrins directly in 600  $\mu\text{L}$  of  $\text{D}_2\text{O}$ . The values of  $\Delta\delta$  caused upon complexation were measured.

### Computational Methods

Molecular dynamics (MD) simulations were performed using the GROMACS package (35) and employing the GROMACS ffgmx force field (36).

The  $\beta\text{CD}$  structure was obtained from the Hetero-compound Information Centre - Uppsala (HIC-Up) online database (37), and that of  $\text{M}\beta\text{CD}$  was built by editing the original  $\beta\text{CD}$  structure and adding the substitution groups. The initial structures of the OME and ARG molecules were supplied as pdb files created in-house. The structures were then converted to GROMACS input files (conformation and topology) using PRODRG (38). The deprotonated form of OME, present in solutions with  $\text{pH} = 10$  (39,40), was addressed by extracting the benzimidazole proton when running PRODRG. A pm3 level optimization of the partial charges distribution for the deprotonated molecule OME and ARG molecules was established using GAMESS (41) and introduced into the respective topology input files.

In summary, pdb files for  $\beta\text{CD}$ ,  $\text{M}\beta\text{CD}$ , OME, and ARG were converted into GROMACS format, with charges established, respectively, resorting to PRODRG (cyclodextrins) and pm3 calculations.

Four systems were used in order to rationalize different aspects observed in the experimental results. In all systems, only one molecule of OME is present. One of the systems is composed by the OME molecule and a single molecule of ARG, so as to assess the specific interactions between the two molecules. In a second model system, 1:6 excess of ARG is present, establishing a closer correspondence to the experimental setup. The interactions between ARG and the inclusion complexes were studied in two separate systems where OME was included in the cavity of  $\beta\text{CD}$  and  $\text{M}\beta\text{CD}$ , respectively, with a 6:1 ratio in ARG molecules to the inclusion complex.

In order to maintain electroneutrality, one sodium ion was introduced in every system. The long range electrostatic interactions were handled by the particle mesh Ewald method (42). The solvent was considered explicitly using the simple point charge water model and an algorithm for rigid water molecules (43). The system was enclosed in a cell with periodic boundary conditions. Smaller cell sizes, not lower than  $30 \times 30 \times 25 \text{ \AA}^3$ , were used for the systems where only OME and ARG were present, including at least 750 water molecules. In systems where cyclodextrins were present, the volume was at least  $33 \times 33 \times 33 \text{ \AA}^3$ , including more than 1,000 water molecules. The simulation was conducted in the NPT ensemble at a constant temperature of 300 K with coupling to an external bath (44).

An equilibration run of at least 3 ns was done previous to the production trajectory runs, without constraints. The formation of the inclusion complex is a result of a pre-equilibration process in the absence of ARG, and equilibration was only considered to be completed upon inclusion. The

production runs were carried for 15 ns in the case of 1:1 OME:ARG and 6 ns for every other system. A time step of 1.5 fs was used throughout.

### RESULTS AND DISCUSSION

Phase solubility diagrams of OME in solution containing ARG and each cyclodextrin are shown in Fig. 2a. Solubility profiles of OME with  $\beta\text{CD}$  (ai) and  $\text{M}\beta\text{CD}$  (a ii) within the concentration range studied displayed a typical AL-type diagram, indicating the formation of 1:1 stoichiometry OME:cyclodextrin inclusion complexes in ARG solution. The OME solubility in ARG aqueous solution was 3.4 mM. In presence of the maximum concentration of  $\beta\text{CD}$ , the solubility of OME presented a 1.9-fold increase (to 6.4 mM) and a 3.7-fold increase when  $\text{M}\beta\text{CD}$  was used (to 12.7 mM).

The  $K_{1:1}$  values for the inclusion complexes formed by OME and the cyclodextrins, in the absence and presence of ARG (Table I), were calculated (1) according to Higuchi and

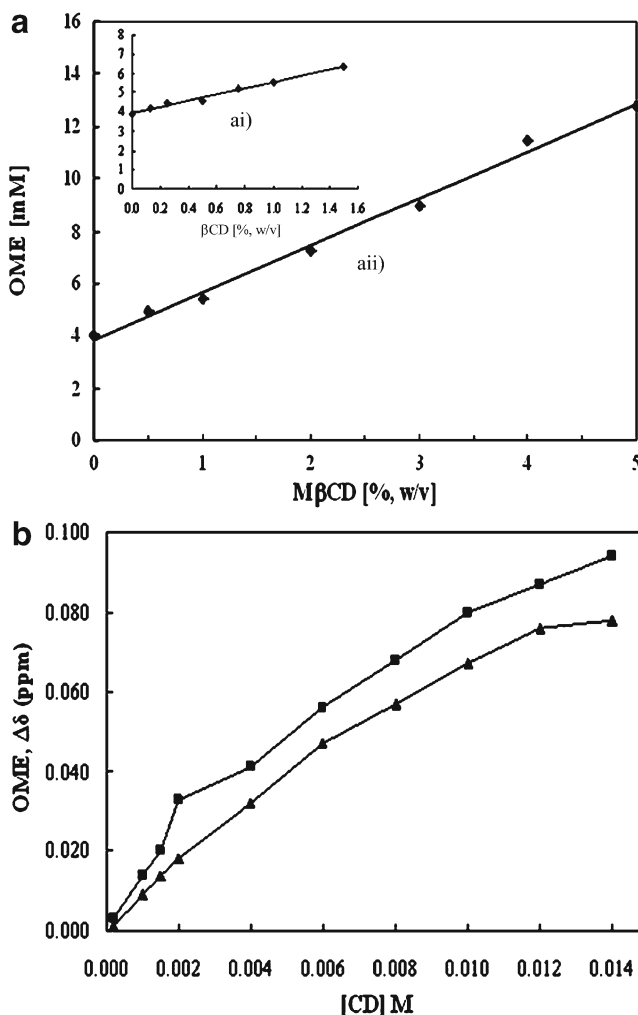


**Fig. 2.** a Phase solubility diagrams of OME: $\beta\text{CD}$  (ai) and OME: $\text{M}\beta\text{CD}$  (a ii) in ARG aqueous solution. b  $^1\text{H-NMR}$  chemical shifts increments of OME ( $\text{CH}_3$  2 group) versus  $\beta\text{CD}$  (triangles) and  $\text{M}\beta\text{CD}$  (squares) increased molar concentrations in ARG aqueous solution

**Table I.** OME Solubility in Presence of CDs with and without ARG ( $S_2$ ), Slope ( $D_2$ ), and  $K_{1:1}$  Values Calculated by Two Different Methods

Inclusion complex	$S_2$ (M, $10^{-3}$ ) <sup>a</sup>	$D_2$ ( $10^{-2}$ ) <sup>b</sup>	$K_{1:1}$ ( $M^{-1}$ )	$K_{1:1}$ (ppm)
OME:βCD	5.8±0.093 <sup>c</sup>	16.9	56.9±2.335 <sup>c</sup>	60.0 <sup>c</sup>
OME:ARG: βCD	6.4±0.008	18.1	65.0±1.495	74.0
OME:MβCD	11.3±0.118 <sup>c</sup>	19.4	77.4±1.388 <sup>c</sup>	90.0 <sup>c</sup>
OME:ARG:MβCD	12.7±0.005	21.4	80.1±1.236	101.6

Each value represents the mean of three determinations ± standard deviation (SD)

<sup>a</sup> OME solubility in CD solutions ( $13.2 \times 10^{-3}$  M βCD and  $42 \times 10^{-3}$  M MβCD) with and without ARG

<sup>b</sup> Slopes of the phase solubility diagrams achieved in inclusion complexes

<sup>c</sup> Results from (11) and used for comparison purposes

Connors (33) and (2) using a nonlinear least squares procedure. For this purpose, we selected the protons of OME that showed the largest  $\Delta\delta$  (Fig. 2b) in the presence of increased concentrations of βCD or MβCD in ARG aqueous solution. The inclusion of OME in the cyclodextrin cavity has been observed to increase the solubility of the former (11). However, the presence of the alkali agent, ARG, increases even more the solubility and  $K_{1:1}$  values for both inclusion complexes.

The increase in  $K_{1:1}$  for the complex OME:βCD was larger than that for OME:MβCD in the presence of ARG (Table I). Note, however, that the complexes formed with MβCD were already more stable before the introduction of the basic amino acid. It should also be noted that these values, calculated by the two independent methods, are similar.

The <sup>1</sup>H-NMR spectra of inclusion complexes in the ARG aqueous solution are presented in Fig. 3, and the discussion follows the labeling presented in the panels of Fig. 1. The  $\Delta\delta$  values for the inclusion complexes are presented in Table II.

In the system OME:ARG (data not shown), it was possible to observe that all protons in both rings of the drug presented larger  $\Delta\delta$  due the presence of ARG, indicating

possible interactions between both compounds. At the same time, ARG presented more accentuated  $\Delta\delta$  in the protons near the amino group, suggesting the involvement of this group.

In general, the changes in  $\Delta\delta$  due to the introduction of ARG in the system are larger for the protons on the OME:βCD complex (Table II) than the changes observed for  $\Delta\delta$  values for the OME:MβCD complex (Table II). This is clearly visible in the ones pertaining to protons located in the included part of OME (Ha, Hb, Hc, and methoxy 2) and in the βCD protons inside the cavity (H3 and H5). The overall behavior is compatible with an increased stabilization of the OME:cyclodextrin complexes due to ARG.

In  $\Delta\delta$  values for the OME protons when complexed with βCD in the absence and the presence of ARG (Table II), significant changes are observed essentially for the portion of the molecule that is inserted in the cyclodextrin cavity (Hb, Hc, and methoxy 2). The  $\Delta\delta$  for methoxy 1 also presents a significant alteration in the presence of ARG. Changes in the protons of the βCD are also observed when ARG is present, specially for protons H5 (larger in absolute value) and H6 (smaller in absolute value). The changes observed for the  $\Delta\delta$  in the protons of the OME in the complex with MβCD are

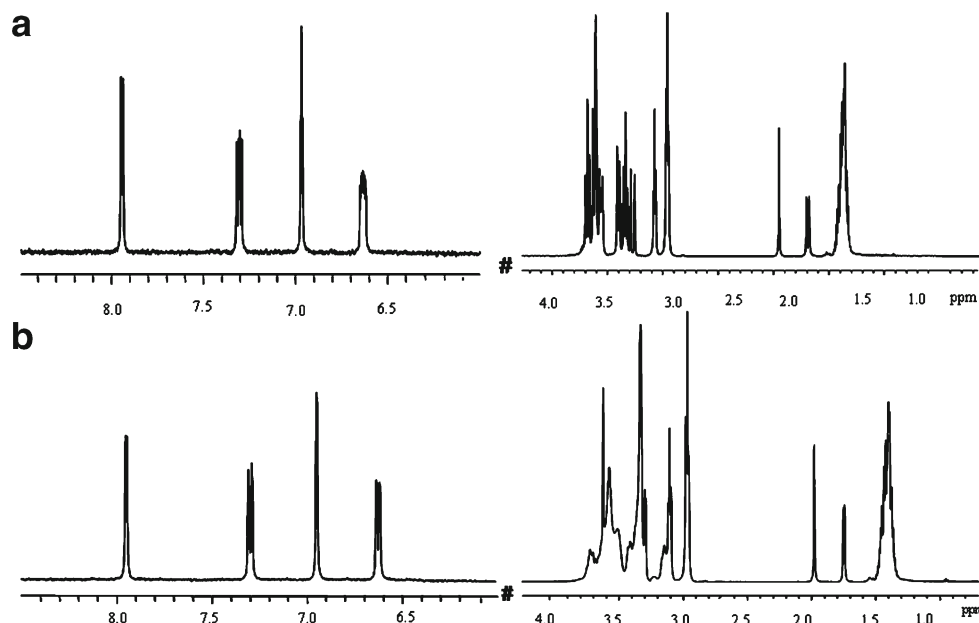


**Fig. 3.** <sup>1</sup>H-NMR spectrum of inclusion complex OME:βCD (a) and inclusion complex OME:MβCD (b) in ARG aqueous solution

**Table II.**  $\Delta\delta$  for the Inclusion Complexes Formed between OME and  $\beta$ CD/M $\beta$ CD in Absence and Presence of ARG Aqueous Solution

Assignment	$\Delta\delta$ ( $\delta_{\text{complexed}} - \delta_{\text{free}}$ )				
	OME	OME: $\beta$ CD <sup>a</sup>	OME: $\beta$ CD:ARG	OME:M $\beta$ CD <sup>a</sup>	OME:M $\beta$ CD:ARG
Ha		-0.001	-0.003	-0.025	-0.020
Hb		-0.015	-0.042	-0.036	-0.045
Hc		-0.005	-0.030	-0.024	-0.033
Hd		0.001	0.010	0.010	0.028
Methoxy 1		-0.023	0.013	-0.025	0.005
Methoxy 2		-0.011	-0.032	-0.026	-0.018
Methyl 1		0.000	0.000	-0.001	0.012
Methyl 2		0.041	0.038	0.060	0.041
$\beta$ CD/M $\beta$ CD					
H1		-0.019	-0.025	-0.049	-0.051
H2		-0.019	-0.026	-0.044	-0.042
H3		-0.054	-0.061	-0.054	-0.072
H4		-0.018	-0.024	-0.020	-0.019
H5		-0.026	-0.050	-0.086	-0.083
H6		-0.041	-0.033	-0.037	-0.035
Methyl-6'		-	-	-0.055	-0.033

<sup>a</sup> Results from (11)

similar for the included and the external part of the molecule (Table II). However, the most significant changes are observed in Hd, methoxy 1, and methyl 2 which are located in the exposed part of OME. The presence of ARG only changes slightly the  $\Delta\delta$  of the protons of M $\beta$ CD except for H3 (larger in absolute value) and methyl 6' (smaller in absolute value).  $\Delta\delta$  of ARG protons show significant alteration in the chemical shift of H<sub>I</sub>, which is more important for the system where M $\beta$ CD is present.

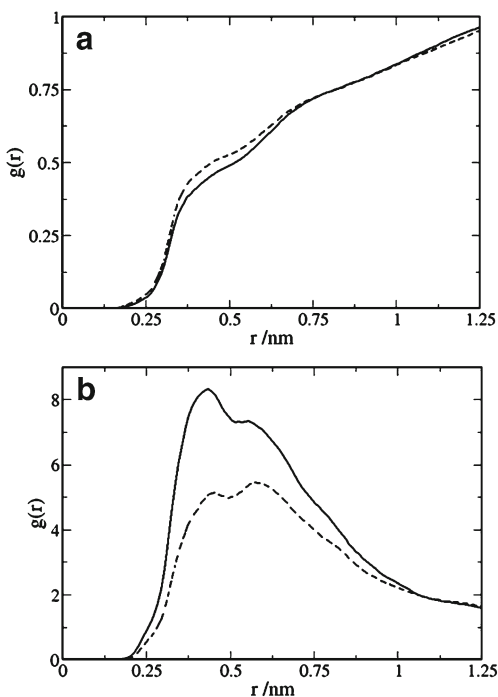


**Fig. 4.** Radial distribution function of water (a) and ARG (b) around the exposed part of OME in the inclusion complex with  $\beta$ CD (full line) and M $\beta$ CD (dashed line)

Regarding the radial distribution function (RDF) of water and ARG around the 6-methoxy-2-((4-methoxy-3,5-dimethylpyridin-2-yl) methylsulfinyl) part of OME, the portion of the molecule not included in the cavity (Fig. 4), it is possible to observe that the RDF for water in the proximity of OME (Fig. 4a) presents smaller values in the OME: $\beta$ CD complex, which are originated by a larger probability density of ARG in the proximity of OME (Fig. 4b).

The structure of the multicomponent inclusion complex formed with  $\beta$ CD is illustrated in the snapshot of Fig. 5. ARG molecules located at the wider side of the cavity minimize the interaction of OME with the solvent, thus increasing the stability of the complex. This effect, although being more significant in the OME: $\beta$ CD complex, is not sufficient to make this complex more stable than the one formed by OME and M $\beta$ CD.

The main reason suggested for the larger stability of the OME:M $\beta$ CD complex in the absence of ARG was the larger protection given to OME by a deeper inclusion in the cavity

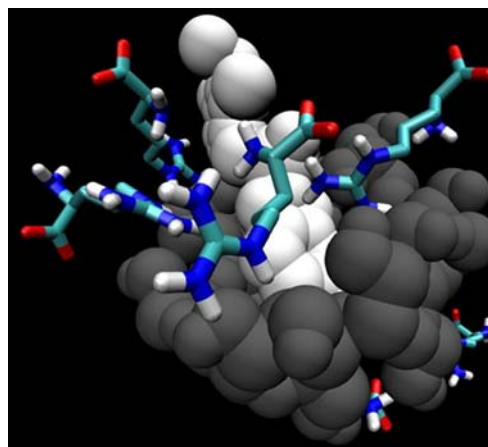


**Fig. 5.** Snapshot from the molecular dynamics simulation of the multicomponent inclusion complex formed between OME (light gray) and  $\beta$ CD (dark gray) in the presence of ARG (colored)

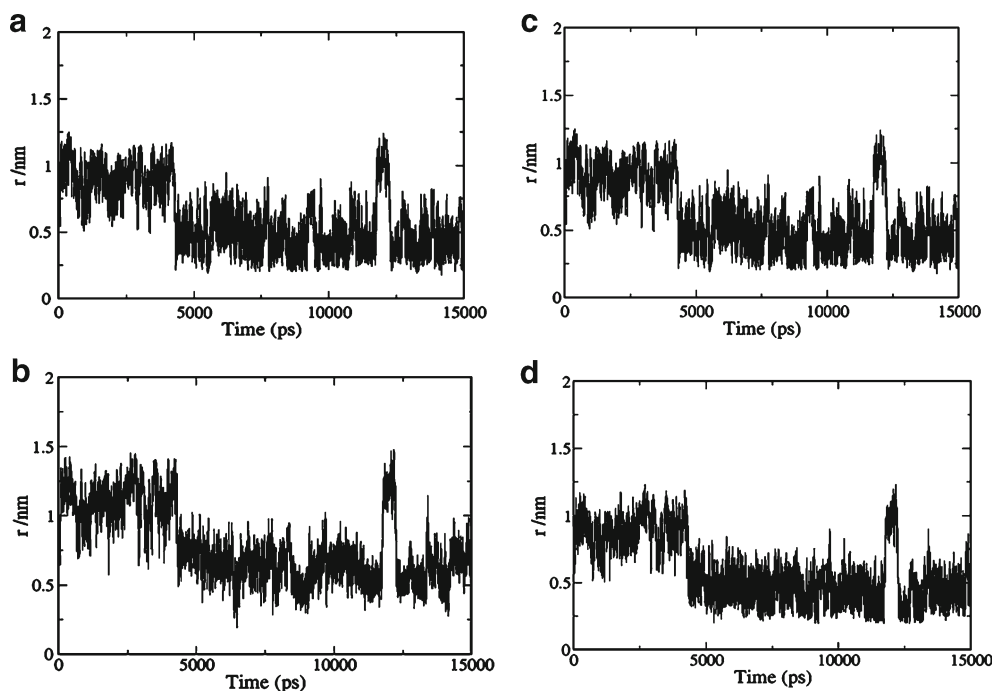


**Fig. 6.** Hydrogen H(c,ARG) (a) and hydrogen H(a,ARG) (b) distances to the N(2,OME) nitrogen and time evolution of the distances H(c,ARG)-N(2,OME) (c) and H(c,ARG)-N(3,OME) (d) along the trajectory

(11). When ARG is present in the system, the difference between the average distance from the e and f atoms of the OME to the center of mass of the O4 atoms of the cyclodextrin that can be considered as a reference to the center of

the cyclodextrin inner cavity of the two complexes is not significant. This can explain to a large extent the large difference observed for the  $\Delta\delta$  in the OME: $\beta$ CD and the small difference in the  $\Delta\delta$  for OME:M $\beta$ CD upon the addition

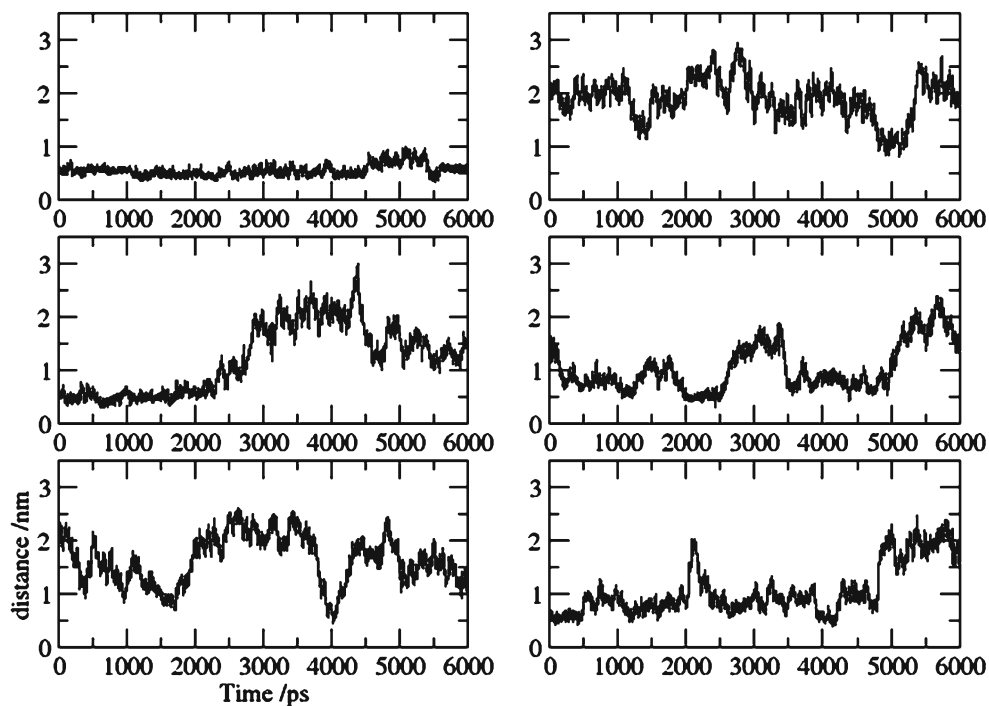


**Fig. 7.** Distance from the center of mass of OME to the center of mass of each ARG molecules along the trajectory in the system where an excess of ARG is present. Each panel corresponds to a different ARG molecule

of ARG, leading to overall similar  $\Delta\delta$  results when the ARG is present. Upon the OME:ARG interaction in aqueous solution, to highlight this interaction, the system is studied in the absence of cyclodextrin. In a first approach, a 1:1 system is inspected to understand how the two molecules interact. In a second approach, a 1:6 excess of ARG is present, to establish a closer correspondence to the experimental setup.

In the system where OME and ARG are in a proportion of 1:1, H(c,ARG) was consistently closer than H(a,ARG) to the nitrogen atom N(2,OME) (Fig. 6). These H(c,ARG)–N(2,OME) distances are very small (approximately 3 Å), and by the residence time in close proximity, we have a clear indication of hydrogen bond formation. Also, H(c,ARG) interacts in a similar fashion with N(2,OME) and N(3,OME) atoms (Fig. 6), leading us to the conclusion that the probability of hydrogen bonding in the two cases is similar. These results are indicative of a direct electrostatic effect in the interaction between ARG and OME in the considered protonation states, and the formation of a hydrogen bond between the region of the largest opposite charge density in each molecule.

Figure 7 shows the distances between the center of mass of OME and the center of mass of each ARG molecule, when a large excess of ARG is present in solution. Superimposing the different panels shows that most of the time, ca. three molecules of ARG located in the proximity of an OME molecule. This large local concentration implies a significant desolvation of the OME molecule, as suggested before, which may be a factor contributing to the larger stability and solubility of OME in the presence of ARG (11).

The combined analysis of the results obtained from NMR and MD studies show that ARG plays an active role in the multicomponent complex formation by having a tendency to be located near the inner ring surface of the cyclodextrin.

## CONCLUSION

NMR experiments and MD simulations were performed for studying the effect of the presence of ARG on the stability of inclusion complexes of OME:cyclodextrin and on the solubility and stability of OME.

Higher values of  $K_{1:1}$  for the OME:cyclodextrin complexes were obtained with the introduction of ARG in the system. Also, an increase in drug solubility in the presence of ARG was recorded. Both these observations have been correlated with a minimization of the contact between the drug and the solvent. Although the increase in solubility is more pronounced in the OME: $\beta$ CD:ARG system, overall, the OME:M $\beta$ CD:ARG still leads to better results.

ARG was observed to play an important role in the increase of drug solubility and stability of free OME molecules. This is mainly attributed to the amino acid, by establishing hydrogen bonds with drug molecules, forcing a significant desolvation of the OME molecule.

Taking into account that improvements in OME solubility and stability are two important parameters to address in drug formulation with better bioavailability, the combination of cyclodextrins and alkali agents, namely ARG, seems suitable to attain this final purpose.

## ACKNOWLEDGMENTS

A.F. would like to acknowledge the grant SFRH/BD/19175/2004, and J.M.G.S. would like to acknowledge the grants SFRH/BD/17440/2004 and SFRH/BPD/46319/2008 from Fundação para a Ciência e Tecnologia (FCT, Portugal). The authors would like to thank Belmac Laboratory, S.A. (Madrid, Spain) for kindly donating of OME and Roquette (Lestrem, France) for providing the cyclodextrins used in this study,  $\beta$ -cyclodextrin, and methyl- $\beta$ -cyclodextrin.

## REFERENCES

1. Karljivic-Rajic K, Novovic D, Marinkovic V, Agbaba D. First-order UV-derivative spectrophotometry in the analysis of omeprazole and pantoprazole sodium salt and corresponding impurities. *J Pharm and Bio Anal.* 2003;32:1019–27.
2. Pérez-Ruiz T, Martínez-Lozano C, Sanz A, Bravo E, Galera R. Determination of omeprazole, hydroxyomeprazole and omeprazole sulfone using automated solid phase extraction and micellar electrokinetic capillary chromatography. *J Pharm and Biom Anal.* 2006;46:100–6.
3. Markovic N, Agotonovic-Kustrin S, Glass B, Prestidge CA. Physical and thermal characterisation of chiral omeprazole sodium salts. *J Pharm and Biom Anal.* 2006;42:25–31.
4. Min DS, Um KA, Kim YS, Park PW. Method for preparing enteric-coated oral drugs containing acid-unstable compounds., U.S. Patent, 1995.
5. Salama F, El-Abasawy N, Abdel-Razeq SA, Ismail MMF, Fouad MM. Validation of the spectrophotometric determination of omeprazole and pantoprazole sodium via their metal chelates. *J Pharm and Biom Anal.* 2003;33:411–21.
6. Shimizu M, Unoa T, Niioaka T, Yaii-Furukori N, Takahata T, Sugawara K, Tateishi T. Sensitive determination of omeprazole and its two main metabolites in human plasma by column-switching high-performance liquid chromatography: application to pharmacokinetic study in relation to CYP2C19 genotypes. *J Chromat B.* 2006;832:241–8.
7. Stroyer A, McGinity JW, Leopold CS. Solid state interactions between the proton pump inhibitor omeprazole and various enteric coating polymers. *J Pharm Sci.* 2005;95:1342–53.
8. Nakagawa T, Immel S, Lichtenthaler FW, Lindner HJ. Topography of the 1:1  $\beta$ -cyclodextrin–nitromethane inclusion complex. *Carb Res.* 2000;324:141–6.
9. Liu Y, Chen G, Chen Y, Lin J. Inclusion complexes of azadirachtin with native and methylated cyclodextrins: solubilization and binding ability. *Bioorg Med Chem.* 2005;13:4037–42.
10. Loftsson T, Brewster ME, Másson M. Role of cyclodextrins in improving oral drug delivery. *Am J Drug Deliv.* 2004;2:1–15.
11. Figueiras A, Sarraguça JMG, Carvalho RA, Pais AACC, Veiga FJB. Interaction of omeprazole with a methylated derivative of  $\beta$ -cyclodextrin: phase solubility, NMR spectroscopy and molecular simulation. *Pharm Res.* 2006;24:377–89.
12. Li J, Xiao H, Li J, Zhongb Y. Drug carrier systems based on water-soluble cationic  $\beta$ -cyclodextrin polymers. *Int J Pharm.* 2004;278:329–42.
13. Loftsson T. Pharmaceutical applications of cyclodextrins. 1. Drug solubilization and stabilization. *J Pharm Sci.* 1996;85:1017–25.
14. Tirapegui C, Jara F, Guerrero J, Rezende MC. Host–guest interactions in cyclodextrin inclusion complexes with solvatochromic dyes. *J Phys Org Chem.* 2006;19:786–92.
15. Fermeglia M, Ferrone M, Lodi A, Prici S. Host–guest inclusion complexes between anticancer drugs and  $\beta$ -cyclodextrin: computational studies. *Carbohydr Polym.* 2003;53:15–44.
16. Bea I, Jaime C, Kollman P. Molecular recognition by  $\beta$ -cyclodextrin derivatives: molecular dynamics, free-energy perturbation and molecular mechanics/Poisson–Boltzmann surface area goals and problems. *Theor Chem Acc.* 2002;108:286–92.

17. Haller J, Kaatze U. Octylglucopyranoside and cyclodextrin in water. Self-aggregation and complex formation. *J Phys Chem B*. 2009;113:1940–7.
18. Nilsson M, Valente AJM, Olofsson G, Söderman O, Bonini M. Thermodynamic and kinetic characterization of host–guest association between bolaform surfactants and  $\alpha$ - and  $\beta$ -cyclodextrins. *J Phys Chem B*. 2008;112:11310–6.
19. Sellner B, Zifferer G, Kornherr A, Krois D, Brinker UH. Molecular dynamics simulations of  $\beta$ -cyclodextrin–aziadaman-tane complexes in water. *J Phys Chem B*. 2008;112:710–4.
20. Thompson DO. Cyclodextrins-enabling excipients: their present and future use in pharmaceuticals. *Crit Rev Therap Drug Carr Syst*. 1997;14:1–104.
21. Duchêne D, Wouessidjewe D. The current state of  $\beta$ -cyclodextrin in pharmaceuticals. *Acta Pharm Technol*. 1990;36:1–6.
22. Mura P, Zerrouk N, Faucci MT, Maestrelli F, Chemtob C. Comparative study of ibuprofen complexation with amorphous beta-cyclodextrin derivatives in solution and in solid state. *Eur J Pharm and Biopharm*. 2002;54:181–91.
23. Boulmedarat L, Bochot A, Lesieur S, Fattal E. Evaluation of buccal methyl- $\beta$ -cyclodextrin toxicity on human oral epithelial cell culture model. *J Pharm Sci*. 2005;94:1300–9.
24. Ventura CA, Giannone I, Paolino D, Pistarà V, Corsaro A, Puglisi G. Preparation of celecoxib-dimethyl- $\beta$ -cyclodextrin inclusion complex: characterization and *in vitro* permeation study. *Eur J Med Chem*. 2005;40:624–31.
25. Garnero C, Longhi M. Study of ascorbic acid interaction with hydroxypropyl- $\beta$ -cyclodextrin and triethanolamine, separately and in combination. *J Pharm and Biom Anal*. 2007;45:536–45.
26. Mura P, Maestrelli F, Cirri M. Ternary systems of naproxen with hydroxypropyl- $\beta$ -cyclodextrin and amino acids. *Int J Pharm*. 2003;260:293–302.
27. Mura P, Bettinetti GP, Cirri M, Maestrelli F, Sorrenti M, Catenacci L. Solid-state characterization and dissolution properties of naproxen–arginine–hydroxypropyl- $\beta$ -cyclodextrin ternary system. *Eur J Pharm and Biopharm*. 2005;59:99–106.
28. Ain-Ai A, Gupta PK. Effect of arginine hydrochloride and hydroxypropyl cellulose as stabilizers on the physical stability of high drug loading nanosuspensions of a poorly soluble compound. *Int J Pharm*. 2008;351:282–8.
29. Manali S, Poonam K, Pankajkumar S, Vikrant V, Yogesh P. Effect of PVP K30 and/or L-arginine on stability constant of etoricoxib–HP $\beta$ CD inclusion complex: preparation and characterization of etoricoxib–HP $\beta$ CD binary system. *Drug Dev Ind Pharm*. 2009;35:118–29.
30. Kolbe I, Csabai K, Szente L, Szejtli J. Development of an omeprazole/arginine/betaCD formulation. 10th International Cyclodextrin Symposium. 2000. p. 337–45.
31. Klokkers K, Kutschera M, Fischer W. Stabilization of acid sensitive benzimidazoles with amino acid/cyclodextrin combinations. U.S. Patent. 1998.
32. Figueiras A, Carvalho RA, Ribeiro L, Torres-Labandeira JJ, Veiga FJB. Solid-state characterization and dissolution profiles of the inclusion complexes of omeprazole with native and chemically modified  $\beta$ -cyclodextrin. *Eur J Pharm and Biopharm*. 2007;67:531–9.
33. Higuchi T, Connors A. Phase-solubility techniques. In: Wiley-Interscience, editors. In advances in analytical chemistry instrumentation. New York: 1965. p. 117–212
34. Tapia MJ, Burrows HD, García JM, García F, Pais AACC. Lanthanide ion interaction with crown ether methacrylic polymer, poly (1, 4, 7, 10-tetraoxacyclododecan-2-methyl methacrylate), as seen by spectroscopy, calorimetric and theoretical studies. *Macromolecules*. 2004;37:856–62.
35. Lindahl E, Hess B, Van der Spoel D. A package for molecular simulation and trajectory analysis. *J Mol Mod*. 2001;7:306–17.
36. Berendsen HJC, Van der Spoel D, Van Drunen R. GROMACS: a message-passing parallel molecular dynamics implementation. *Comput Phys Commun*. 1995;91:43–56.
37. Kleywegt GJ, Jones TA. Databases in protein crystallography. *Acta Crystallogr Sect D-Biol Crystallogr*. 1998;D54:1119–31.
38. Schuettelkopf AW, Van Aalten DMF. PRODRG—a tool for high throughput crystallography of protein–ligand complexes. *Acta Crystallogr Sect D-Biol Crystallogr*. 2004; D60:1355–63.
39. Brändström A, Bergman NA, Grundevik I, Johansson S, Ohlson L. Chemical reactions of omeprazole and omeprazole analogues. II. Kinetics of the reaction of omeprazole in the presence of 2-mercaptoethanol. *Acta Chem Scand*. 1998;43:549–68.
40. Yang R, Zavala SG, Schulman PJ. Acid–base chemistry of omeprazole in aqueous solutions. *Anal Chim Acta*. 2003;481:155–64.
41. Schmidt MW, Baldrige KK, Boatz JA, Elbert ST, Gordon MS, Jensen JH, *et al.* General atomic and molecular electronic-structure system. *J Comput Chem*. 1993;14:1347–63.
42. Essman U, Perela L, Berkowitz ML, Darden T, Lee H, Pedersen LG. A smooth particle mesh Ewald method. *J Chem Phys*. 1995;103:8577–92.
43. Miyamoto S, Kollman PA. Settle: an analytical version of the shake and rattle algorithms for rigid water models. *J Comput Chem*. 1992;13:952–62.
44. Berendsen HJC, Postma JPM, DiNola A, Haak J. Molecular dynamics with coupling to an external bath. *J Chem Phys*. 1984;81:3684–90.